An investigation on 4-thiazolidinone derivatives as dual inhibitors of aldose reductase and protein tyrosine phosphatase 1B, in the search for potential agents for the treatment of type 2 diabetes mellitus and its complications

Rosanna Maccari,[a]* Antonella Del Corso,[b] Paolo Paoli,[c] Ilenia Adornato,[a] Giulia Lori,[c] Francesco Balestri,[b] Mario Cappiello,[b] Alexandra Naß,[d] Gerhard Wolber,[d] Rosaria Ottanà[a]

[a] *Department of Chemical, Biological, Pharmaceutical and Environmental Sciences, University of Messina, Polo Universitario Annunziata, Viale SS. Annunziata, 98168 Messina, Italy*

[b] *Department of Biology, Biochemistry Unit, University of Pisa, Via S. Zeno, 51, 56123 Pisa, Italy*

[c] *Department of Scienze Biomediche Sperimentali e Cliniche, Sezione di Scienze Biochimiche, University of Firenze, Viale Morgagni 50, 50134 Firenze, Italy*

[d] *Institute of Pharmacy, Computer-Aided Molecular Design, Freie Universitaet Berlin, Koenigin-Luisestr. 2+4, 14195 Berlin, Germany*

* Corresponding author – email: rmaccari@unime.it

Abstract – Designed multiple ligands (DMLs), developed to modulate simultaneously a number of selected targets involved in etiopathogenetic mechanisms of a multifactorial disease, such as diabetes mellitus (DM), are considered a promising alternative to combinations of drugs, when monotherapy results to be unsatisfactory. In this work, compounds **1-17** were synthesized and in vitro evaluated as DMLs directed to aldose reductase (AR) and protein tyrosine phosphatase 1B (PTP1B), two key enzymes involved in different events which are critical for the onset and progression of type 2 DM and related pathologies. Out of the tested 4-thiazolidinone derivatives, compounds **12** and **16**, which exhibited potent AR inhibitory effects along with interesting inhibition of PTP1B, can be assumed as lead compounds to further optimize and balance the dual inhibitory profile. Moreover, several structural portions were identified as features that could be useful to achieve simultaneous inhibition of both human AR and PTP1B through binding to non-catalytic regions of both target enzymes.

Keywords: diabetes mellitus; designed multiple ligands; 4-thiazolidinone derivatives; aldose reductase; protein tyrosine phosphatase 1B.

Diabetes mellitus (DM) is a multifactorial chronic disease characterized by hyperglycaemia and metabolic dysfunctions. According to WHO reports, currently DM affects more than 420 million people worldwide, being responsible for about 1.5 million deaths every year.[1] The number of people affected by DM is expected to rise to 592 million by 2035, but it might be underestimated since, in the last years, previous estimates have been surpassed.[2] The prevalence of DM is growing, in both industrialized and developing countries, mainly as a consequence of the dramatic incidence of type 2 DM (T2DM) which accounts for more than 90% cases of diabetes worldwide. Obesity, overweight, unbalanced diet and unhealthy lifestyles are the main factors associated with increased risk of T2DM.

In diabetes, hyperglycaemia is a critical condition that originates from insulin deficiency (particularly in type 1 DM) and/or reduced sensitivity of target tissues to the hormone (insulin-resistance, which is a typical feature of T2DM). Hyperglycaemia triggers a number of mechanisms and abnormal cellular signalling, including inflammatory response, increased oxidative stress, lipid peroxidation, altered osmotic balance. On the whole, these hyperglycaemia-induced cellular dysfunctions are responsible for vascular and nervous lesions which underlie the development of serious chronic complications associated to DM, such as neuropathy, nephropathy, retinopathy, atherosclerosis, increased risk of cardiovascular pathologies.[3]

Despite the availability of different effective therapeutic agents, in diabetic patients the control of hyperglycaemia and the prevention of chronic complications by drug monotherapy remain often unsatisfactory. Therefore, an adequate therapeutic management of T2DM is often achieved by means of combinations of drugs acting with different and generally complementary mechanisms of action.

However, combination therapy may be associated with unwanted drug-drug interactions, inappropriate pharmacokinetics, toxicity and scarce patient compliance. In order to overcome the problems related to the polypharmacological approach, the development of "designed multiple ligands" (DMLs) has been recently proposed as a promising strategy which could provide novel drug candidates for the treatment of multifactorial diseases, such as T2DM. DMLs are compounds that have been rationally designed to modulate two or more specific targets which are involved in the etiopathology of a disease, thus possibly resulting in improved efficacy and minor risks compared to both monotherapy and drug combinations.[4-8]

The design of DMLs as potential drugs poses substantial challenges to medicinal chemists, particularly: i) the selection of suitable biological targets, which must be well-characterized and share common structural features, ii) the optimization of the molecular properties in order to obtain drug-like candidates, endowed with an appropriate balance between their multiple

actions. Although DMLs are often low-affinity ligands towards the selected targets, it has been proposed that the even partial inhibition of selected multiple enzymes can result in effective multi-target drugs.[4,6]

In the multifactorial etiopathology of T2DM as well as in the onset and progression of diabetic complications several druggable targets are involved.

Among them, protein tyrosine phosphatase 1B (PTP1B, E.C. 3.1.3.48) is an enzyme crucially implicated in the development of insulin-resistance, which is a characteristic condition in both T2DM and obesity. This enzyme functions as a negative regulator of insulin action, by dephosphorylating specific residues of phosphotyrosine (pTyr) of the activated insulin receptor and thus interrupting the signalling pathways mediated by the hormone. PTP1B also downregulates the signal of leptin, an adipocyte-derived hormone that controls food intake and increases energy expenditure.[9,10] PTP1B overexpression is strictly related to insulin-resistance and it has been demonstrated that the inhibition or genetic ablation of this phosphatase can improve glucose homeostasis, cellular sensitivity to both insulin and leptin, and resistance to diet-induced obesity, without inducing hypoglycaemia or toxic effects.[9-15]

In the complex network of hyperglycaemia-induced dysfunctions that underlie the development of long-term diabetic complications, the enzyme aldose reductase (AR, E.C. 1.1.1.21) plays pivotal roles. Under hyperglycaemic conditions, this aldo-keto reductase catalyses the NADPH-dependent reduction of an excess amount of glucose to sorbitol, which in turn is oxidized to fructose by sorbitol dehydrogenase, in the polyol pathway. The increased consumption of glucose through this pathway leads to osmotic and redox imbalances, increased oxidative stress, and protein alterations.[3,16,17] Moreover, AR can metabolize glutathione-conjugates of reactive unsaturated aldehydes which originate from oxidative stress-induced lipid peroxidation. These reactions represent a step in the overall detoxification pathway of toxic aldehydes, that starts with the glutathione S-transferase-catalyzed adduct formation.[18] However, 3-glutathionyl-1,4-dihydroxynonane, generated by the reductive action of AR on 3-glutathionyl-4-hydroxynonanal, is a pro-inflammatory molecule which can trigger inflammatory signalling, thus contributing significantly to tissue and vascular damage.[17,19] It is well-documented that the inhibition of AR can prevent or slow down the development of chronic diabetic complications (particularly neuropathies, kidney failure, blindness, atherosclerosis, and cardiovascular diseases) as well as can control DM-associated subclinical tissue inflammation. On this basis, AR is considered an emerging target for therapeutic interventions in different pathologies associated with increased inflammatory response, such as diabetes and its complications.[17,19-21]

Because of their functional features, both PTP1B and AR can be assumed as molecular targets of dual inhibitors designed as novel molecules capable to counteract simultaneously two different coexisting pathogenic mechanisms which are crucial for the onset and progression of T2DM and its chronic complications. To our knowledge, so far only a series of potential dual AR/PTP1B inhibitors were designed, starting from a number of flavonoids and naphthoquinones.[22]

Herein, starting from our structure-activity relationship (SAR) studies performed on numerous 4-thiazolidinone derivatives active as AR or PTP1B inhibitors,[23-36] we report the evaluation of a series of (5-arylidene-4-oxo-2-thioxothiazolidin-3-yl)acetic acids and 2-oxo/phenylimino analogues (**1-17**) (Table 1) as dual AR/PTP1B inhibitors. Our previous SAR studies[23-36] highlighted that the pharmacophores of these inhibitors of AR and PTP1B share several structural features that make possible the design of potential dual inhibitors: i) a polar portion, including an acidic moiety or H-bond acceptor groups, which can strongly interact with the positively charged region of the catalytic sites of both enzymes; ii) a lipophilic moiety, generally containing an aromatic system, which can bind hydrophobic amino acid residues lining the lipophilic specificity pocket of AR (such as Trp111, Thr113, Phe122, Ala299, Leu300, Ser302) and the phosphate-binding secondary non-catalytic pocket of PTP1B (such as Arg24, Ala27, Arg254, Met258, Gly259). It is worth pointing out that the 4-thiazolidinone scaffold appears to be capable to maintain a proper orientation of these crucial portions to effectively bind each enzyme and, at the same time, can establish useful interactions which may contribute to stabilize the complex enzyme/inhibitor.[23-36]

Therefore, starting from a "knowledge-based" approach, we merged pharmacophoric elements of inhibitors directed to each of the selected enzymes, maintaining the shared 4-thiazolidinone core. In particular, we decided to insert on the N-3 of the thiazolidinone scaffold an acetic chain, which had been shown to be critical to achieve strong AR inhibition[23-30] and might also be suitable to interact with the positively charged catalytic centre of PTP1B. Different substituents were inserted in the 5-arylidene portion in order to modulate the inhibitory activity. Moreover, it must be taken into consideration that the substitution pattern of the 5-arylidene portion may influence the capability of inhibitors to interact with allosteric regions on the enzyme surface, thus leading to different mechanisms of inhibition, as observed for 4-[(5-arylidene-4-oxo-2-thioxothiazolidin-3-yl)methy]benzoic acids that we have recently reported as allosteric PTP1B inhibitors.[36]

Previously, we had evaluated (5-arylidene-4-oxo-2-thioxothiazolidn-3-yl)acetic acids **1-9** as AR inhibitors (ARIs) of the enzyme extracted from bovine lens.[29,30] In this work, all compounds **1-17** were tested against human recombinant AR and human recombinant PTP1B.

(5-Arylidene-4-oxo-2-thioxothiazolidin-3-yl)acetic acids (**1**-**13**, Table 1) were obtained in high yields by the Knoevenagel condensation of (4-oxo-2-thioxothiazolidin-3-yl)acetic acid with appropriate aldehydes, in refluxing glacial acetic acid and sodium acetate (Scheme 1).

2,4-Thiazolidinediones **14**-**16** (Table 1) were synthesised starting from the Knoevenagel condensation of commercial 2,4-thiazolidinedione with the corresponding aldehydes, in refluxing ethanol and in the presence of piperidine as a base, followed by N-alkylation with bromoacetic acid (Scheme 2).

The synthesis of 2-phenylimino analogue **17** was performed according to a multistep procedure starting from the reaction of phenyl isothiocyanate with glycine. The subsequent reaction between (3-phenylthioureido)acetic acid and chloroacetyl chloride in refluxing ethanol provided (4-oxo-2-phenyliminothiazolidin-3-yl)acetic acid, which was condensed with 3-methoxy-4-benzyloxybenzaldehyde to obtain compound **17** (Scheme 3).

The structures of all compounds were unambiguously assigned by means of analytical and ^{1}H and ^{13}C NMR spectroscopy data. NMR spectra highlighted that compounds **1**-**17** were obtained only as *Z* isomers, in analogy to previously investigated 5-arylidene-4-thiazolidinone derivatives which had been characterized by means of X-ray crystallography.[23,37]

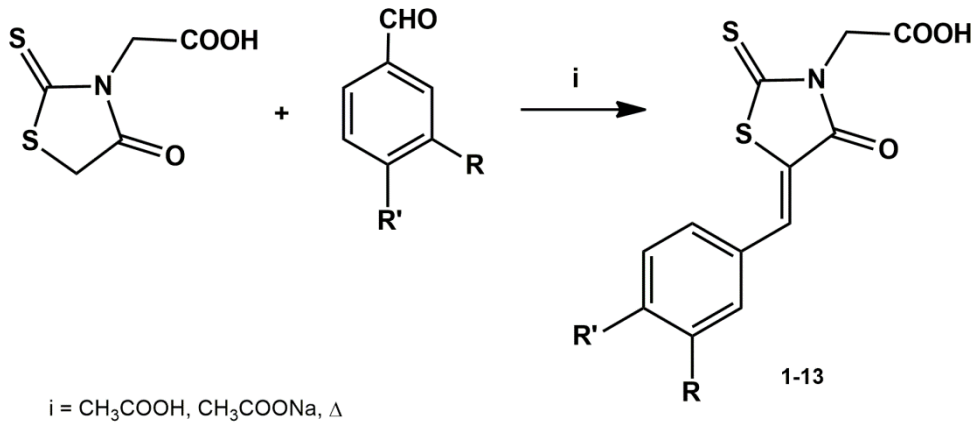

Scheme 1

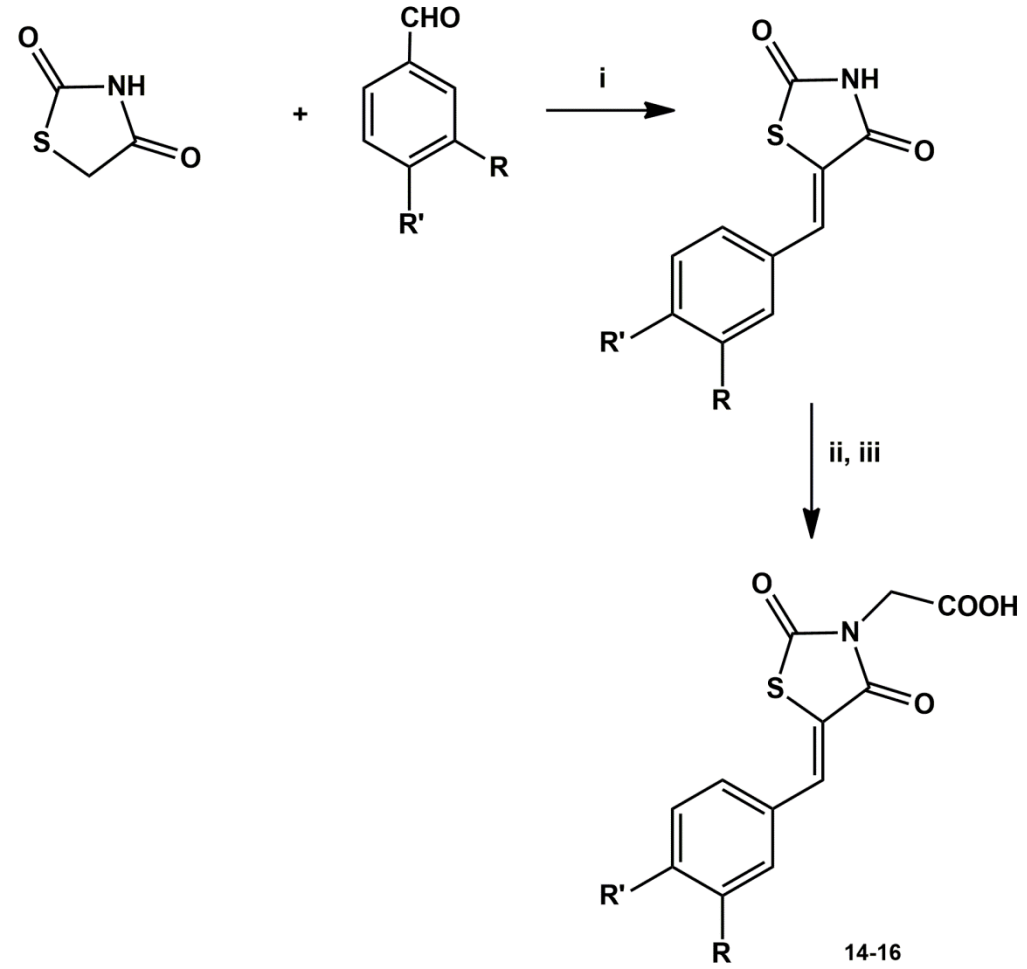

i = piperidine, EtOH, △; ii = $BrCH_2COOH$, K_2CO_3, acetone, △; iii = HCl

Scheme 2

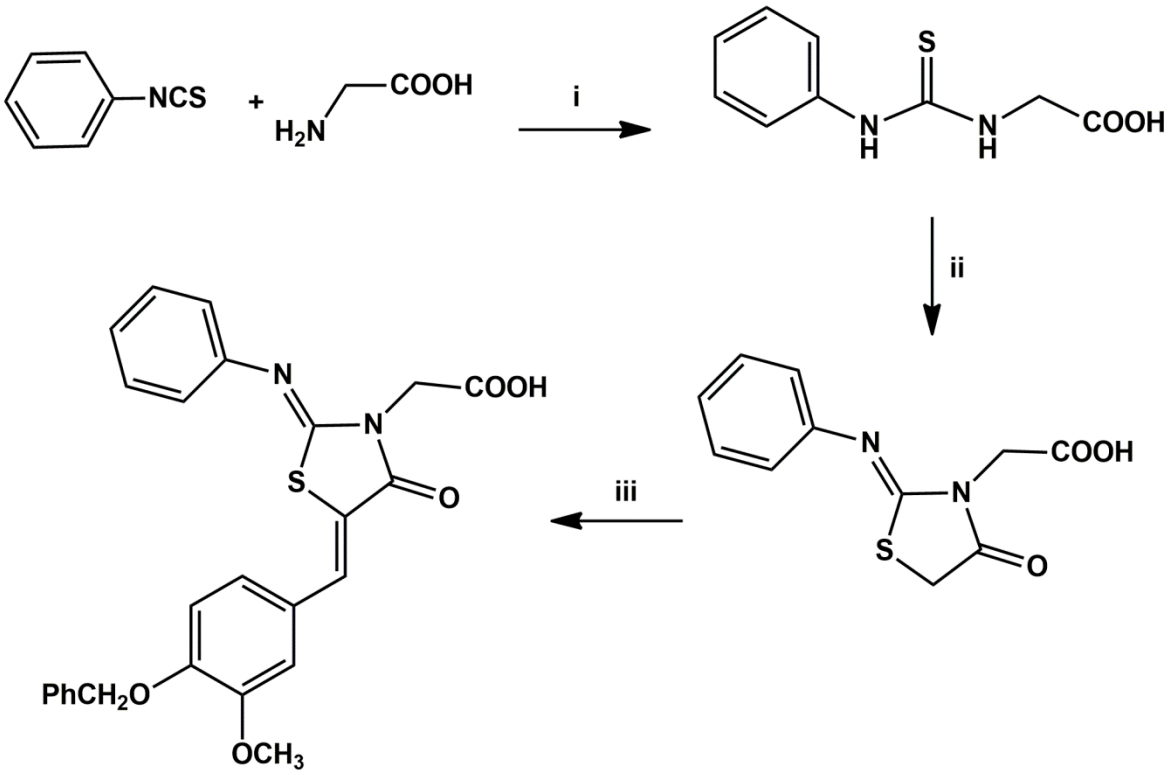

17

i = EtOH, ∆; ii = $ClCH_2COCl$, Et_3N, EtOH, ∆; iii = 4-benzyloxy-3-methoxybenzaldehyde, piperidine, EtOH, ∆.

Scheme 3

The in vitro inhibitory activity of compounds **1**-**17** was assessed both against the human recombinant AR, by using L-idose as substrate[38,39] and Epalrestat as reference drug, and against human recombinant PTP1B, by using *p*-nitrophenyl phosphate as substrate and sodium metavanadate as reference drug. Table 1 reports the IC_{50} values of the tested compounds for the two target enzymes.

Concerning to AR inhibition, all tested 4-thiazolidinone derivatives exhibited excellent inhibitory effects against the human enzyme, with IC_{50} values in the range 0.025 μM-1.41 μM (Table 1), thus resulting in some cases more efficient than Epalrestat (IC_{50} = 0.102 μM). Moreover, except for compound **17**, the IC_{50} values resulted of the same order of magnitude as the enzyme concentration in the assay (67 nM), thus leading these compounds to be considered as "tight binding inhibitors". Relatively to compounds **1**-**9**, these results appeared well comparable with the inhibitory ability displayed against bovine lens AR, using D,L-glyceraldehyde as substrate.[29,30] Also in that case, in fact, taking into account of the higher concentration of the enzyme in the assay (173 nM),[29,30] due to the lower specific activity of the bovine lens enzyme with respect to that of human AR, these powerful ARIs appeared to act as "tight binding inhibitors".

In agreement with previously observed SARs,[29,30] (5-arylidene-4-oxo-2-thioxothiazolidin-3-yl)acetic acids **11**-**13** were shown to be from 3- to almost 10-fold more potent inhibitors of human AR than corresponding 2,4-thiazolidinediones **14**-**16** (Table 1). On the other hand, the replacement of the thiocarbonyl or carbonyl group in position 2 of the thiazolidinone scaffold of compounds **13** and **15** with a 2-phenylimino moiety (derivative **17**, IC_{50} = 1.41 μM) produced a marked reduction of the AR inhibitory effect, leading to an IC_{50} value which was 35-fold and 4-fold higher than those of analogues **13** and **15**, respectively (Table 1).

Among 2-thioxo-4-thiazolidinones **1**-**13** and 2,4-thiazolidinediones **14**-**16**, the influence of the 5-arylidene moiety on the AR inhibitory effectiveness appeared moderate, since their IC_{50} values were included in a rather narrow submicromolar range. However, the presence of a substituent in the *meta* position of the 5-benzylidene ring was generally more beneficial for the inhibition of the target enzyme than the *para*-substitution (Table 1).

The inhibitory effectiveness of compounds **1**-**17** towards human PTP1B was significantly lower when compared to AR inhibition (Table 1). However, the most potent PTP1B inhibitors **16** and **17** exhibited appreciable effectiveness, with IC_{50} values of 12.4 μM and 10.6 μM, respectively; less effective compounds **1**-**4** and **11**-**14** displayed IC_{50} values ranging from 32.5 μM (compound **12**) to 86.8 μM (compound **2**), whereas compounds **6**-**10** and **15** displayed scarce activity, with IC_{50} values higher than 100 μM (Table 1).

Table 1 – Inhibitory activities of compounds **1-17** against human PTP1B and human AR, expressed as IC_{50} (μM).

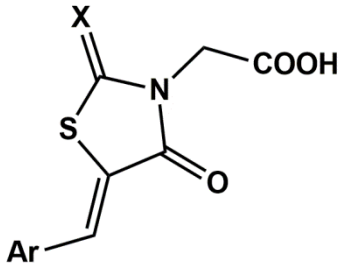

Compd.	*X*	*Ar*	*PTP1B* IC_{50} *(μM)* [a]	*AR* IC_{50} *(μM)* [a]
1	S	4-OC_6H_5-C_6H_4	63.9 ± 2.0	0.060 ± 0.004
2	S	3-OC_6H_5-C_6H_4	86.8 ± 3.2	0.025 ± 0.002
3	S	4-$OCH_2C_6H_5$-C_6H_4	56.0 ± 1.0	0.052 ± 0.003
4	S	3-$OCH_2C_6H_5$-C_6H_4	43.1 ± 1.5	0.053 ± 0.004
5	S	3-OCH_3-C_6H_4	n.d.	0.078 ± 0.007
6	S	4-OCH_2CONH_2-C_6H_4	10 % [b]	0.194 ± 0.011
7	S	3-OCH_2CONH_2-C_6H_4	716.5 ± 136	0.064 ± 0.005
8	S	3-OCH_3,4-OCH_2CONH_2-C_6H_3	378 ± 23	0.228 ± 0.012
9	S	4-OCH_3,3-OCH_2CONH_2-C_6H_3	679 ± 184	0.139 ± 0.011
10	S	C_6H_5CH=CH	171 ± 27	0.125 ± 0.009
11	S	4-$O(CH_2)_2C_6H_5$-C_6H_4	49.4 ± 1.0	0.104 ± 0.010
12	S	3-$O(CH_2)_2C_6H_5$-C_6H_4	32.5 ± 1.1	0.056 ± 0.006
13	S	3-OCH_3,4-$OCH_2C_6H_5$-C_6H_3	54.1 ± 1.0	0.040 ± 0.004
14	O	4-$O(CH_2)_2C_6H_5$-C_6H_4	63.8 ± 2.6	0.364 ± 0.049
15	O	3-OCH_3,4-$OCH_2C_6H_5$-C_6H_3	151 ± 51	0.323 ±0.033
16	O	3-$O(CH_2)_2C_6H_5$-C_6H_4	12.4 ± 0.8	0.276 ± 0.029
17	=NPh	3-OCH_3,4-$OCH_2C_6H_5$-C_6H_3	10.6 ± 0.4	1.41 ± 0.126
Epalrestat				0.102 ± 0.005
Vanadate			0.4 ± 0.01	

[a] Values are expressed as the mean ± S.E.M (see methods for details).
[b] Percent inhibition in the presence of compound **6** at the concentration of 300 μM.
n.d. = not determined.

The presence of a more extended aromatic substituent on the 5-benzylidene ring was generally related to enhanced inhibitory potency, whereas smaller and/or more polar substituents (such as in compounds **6**-**10**) were detrimental for PTP1B inhibition. Interestingly, as observed for AR inhibition, the substitution on the *meta* position of the 5-benzylidene ring was generally more beneficial for the PTP1B inhibitory effectiveness than the substitution in the *para* position (compound **4** vs. **3**, **12** vs. **11** and **16** vs. **14**). This latter SAR appears to be in analogy with SARs observed for certain 4-[(5-arylidene-4-oxo-2-thioxothiazolidin-3-yl)methyl]benzoic acids active as mixed non-competitive PTP1B inhibitors that we recently reported[36]; conversely, in the case of 4-[(5-arylidene-2-arylimino/oxo-4-oxothiazolidin-3-yl)methyl]benzoic acid derivatives that are active as competitive PTP1B inhibitors, the *para*-substitution on 5-benzylidene ring was found to be more beneficial than the *meta*-substitution by providing higher inhibition levels.[31-36]

It is worth noting that the effect of the substituent in position 2 of the 4-thiazolidinone scaffold in modulating the PTP1B inhibitory activity could not be clearly defined, unlike what was observed for AR inhibitory effects. For instance, 2,4-thiazolidinedione **16** was about 3-fold more potent than its 2-thioxo analogue **12**; conversely, 2-thioxo-4-thiazolidinone derivative **13** was about 3-fold more active than its 2,4-thiazolidinedione counterpart **15**. In addition, the replacement of the thiocarbonyl (compounds **13**) or carbonyl group (compound **15**) with a phenylimino moiety (compound **17**) provided an appreciable gain in potency toward PTP1B, with a 5-fold and 14-fold decrease of the IC_{50} value, respectively.

Considering that, among the tested 4-thiazolidinones, compounds **12** and **16** displayed an appreciable dual action in inhibiting both AR and PTP1B, they were further characterized for their kinetic features on both target enzymes.

The kinetic characterization of these molecules had to take into account the remarkable difference in their inhibitory potencies toward AR and PTP1B, thus requiring different analytical approaches.

Firstly, additional tests were performed in order to verify if selected compounds **12** and **16** were reversible or irreversible inhibitors. For PTP1B, appropriate aliquots of the enzyme were incubated in the presence of saturating concentration of each inhibitor for 60 minutes at 37°C. Then, the enzyme mixtures were diluted with assay buffer, and the residual enzyme activity was determined. It was found that the recovery of enzyme activity was complete, suggesting that compounds **12** and **16** behave as reversible PTP1B inhibitors. In the case of AR, being the compounds tight binding inhibitors, active at concentrations comparable to those of the enzyme, it was necessary to perform an extensive dialysis of the enzyme-inhibitor mixture. The

recovery of approximately 70 % of AR activity from a fully inhibited enzyme clearly indicated that both compounds **12** and **16** also behaved as reversible inhibitors toward AR.

In order to determine the action mechanism of these reversible inhibitors, in the case of AR, the effect of the inhibitors was evaluated at different substrate concentrations (Figures 1A and 2A). When fitted by a nonlinear regression analysis to the Morrison equation (see eq. 2 Supplementary material), the apparent inhibition constants (K_i^{app}) were determined. The fitting by nonlinear regression analysis of K_i^{app} as a function of substrate concentration (Figures 1B and 2B) into a general equation of tight binding non-competitive inhibition model (see eq. 3 Supplementary material) allowed the evaluation of the true inhibition constants K_i and K_i'. Thus, while K_i values (asymptote/ordinate intercept) could be estimated being higher than 0.3 µM and 0.5 µM for compounds **12** and **16**, respectively, at least fifty-fold lower values for K_i' (abscissa asymptote) were determined (Table 2). This suggests that both the analysed compounds can be considered as uncompetitive inhibitors.

In the case of PTP1B, reaction rate values at different inhibitor concentrations were analysed by double reciprocal plots. Both compounds **12** and **16** displayed a pure non-competitive mechanism of action (Figures 3A and 4A, respectively). A unique value of dissociation constant for both EI and ESI emerged for each inhibitor (12.0 ± 1.2 µM and 13.1 ± 2.8 µM, for compounds **12** and **16,** respectively), when secondary plots of K_M/Vmax versus the inhibitor concentration were analysed (Figures 3B and 4B, respectively).

Being compound **17** the most active inhibitor for PTP1B, its mechanism of action was also analysed. This compound, as occurred for compounds **12** and **16**, also acted as reversible inhibitor. The reaction rate measurements at different substrate concentrations and at concentrations of compound **17** (Figure 5) revealed for this inhibitor a mixed non-competitive mechanism of action. The K_i and K'_i dissociation constants, evaluated from secondary plots (as above) were 7.6 ± 0.5 µM and 40.6 ± 6.3 µM, respectively, suggesting a preferential binding of compound **17** for the free enzyme.

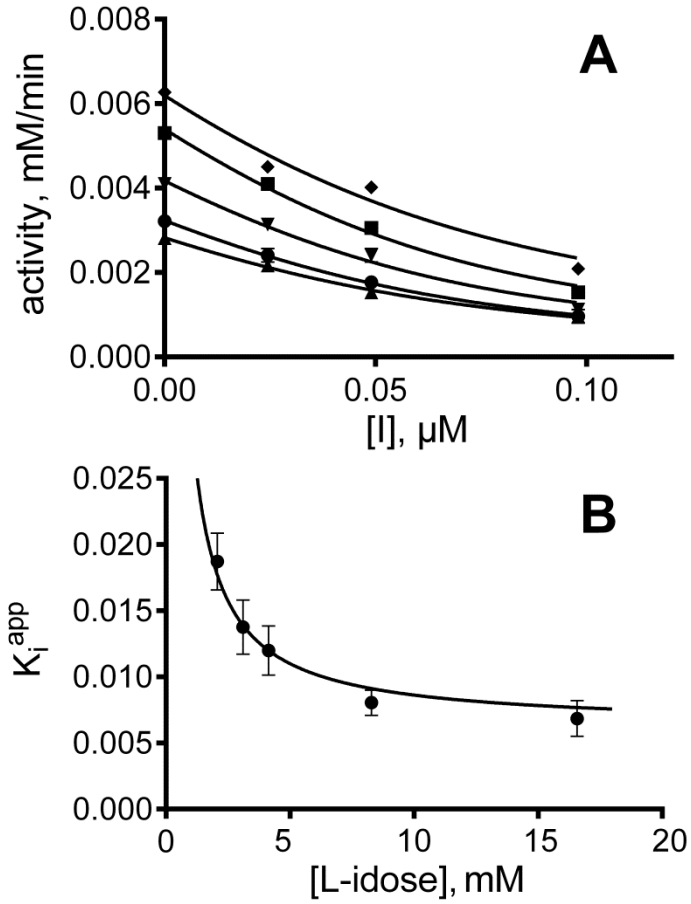

Figure 1. Kinetic characterization of compound **12** as AR inhibitor. **A)** The activity of the purified enzyme (7 mU), expressed as mM/min, was measured at the indicated concentrations of the inhibitor in the presence of the following L-idose concentrations: (▲) 2.1 mM, (●) 3.1 mM, (▼) 4.1 mM, (■) 8.3 mM, (♦) 16.6 mM. Curves were plotted by non linear regression analysis fitting the experimental data to Morrison equation (see Eq. 2 Supplementary material). **B)** The apparent inhibition constants, K_i^{app} determined from Panel A for each substrate concentration were plotted against substrate concentration and fitted by non linear regression analysis to the equation 3 (see Supplementary material) relative to a general case of tight binding non-competitive inhibition model.

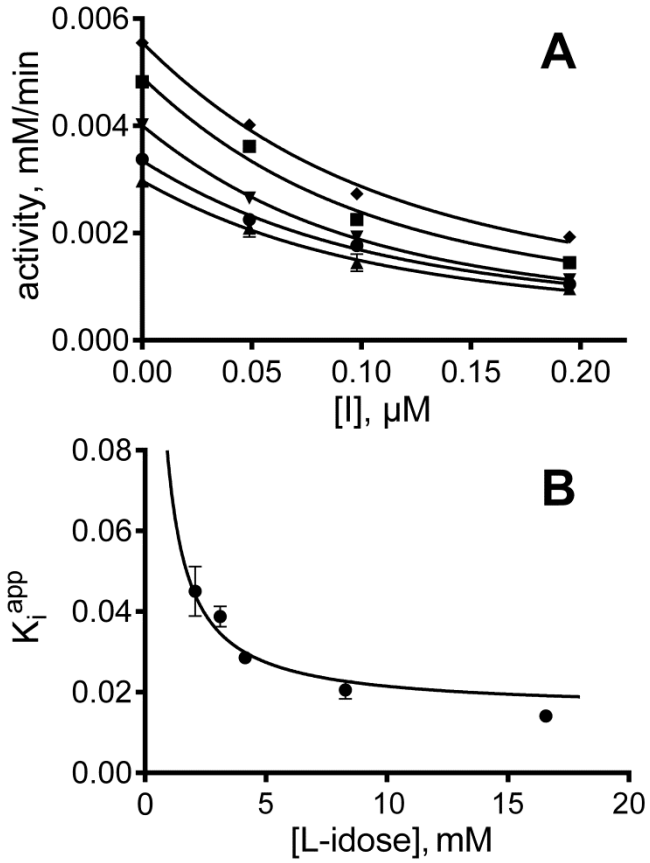

Figure 2. Kinetic characterization of compound **16** as AR inhibitor. **A)** The activity of the purified enzyme (7 mU), expressed as mM/min, was measured at the indicated concentrations of the inhibitor in the presence of the following L-idose concentrations: (▲) 2.1 mM, (●) 3.1 mM, (▼) 4.1 mM, (■) 8.3 mM, (♦) 16.6 mM. Curves were plotted by non linear regression analysis fitting the experimental data to Morrison equation (see Eq. 2 Supplementary material). **B)** The apparent inhibition constants, K_i^{app} determined from Panel A for each substrate concentration were plotted against substrate concentration and fitted by non linear regression analysis to the equation 3 (see Supplementary material) relative to a general case of tight binding non-competitive inhibition model.

Table 2 – Kinetic characterization of compounds **12** and **16** as dual AR/PTP1B inhibitors

	Compound 12		
	Inhibition model	K_i (μM)	K_i' (μM)
AR	Uncompetitive	> 0.3	0.0062 (0.0056– 0.0069)[a]
PTP1B	Non-competitive	12.0 ± 1.2	12.0 ± 1.2
	Compound 16		
	Inhibition model	K_i (μM)	K_i' (μM)
AR	Uncompetitive	> 0.5	0.016 (0.013 – 0.018)[a]
PTP1B	Non-competitive	13.1 ± 3.9	13.1 ± 3.9

[a] 95% confidence limit

The pure or mixed non-competitive mechanism of PTP1B inhibition produced by compounds **12**, **16** and **17** appears to be consistent with the absence of the residue of the 4-methylbenzoic acid that, in our previously reported 4-[(5-arylidene-4-oxothiazolidin-3-yl)methy]benzoic acid derivatives,[31-36] was generally shown to act as a phosphotyrosine-mimetic group with an important role in the anchoring of these inhibitors into the PTP1B catalytic site. Considering that preliminary assays (data not shown) had indicated that the 4-methylbenzoic acid residue was detrimental for AR inhibitory effect, probably because it is not optimal to fit into the rigid polar subsite of the AR catalytic pocket, it was replaced by the residue of acetic acid in compounds **1**-**17**. This led to PTP1B inhibitors, such as compounds **12**, **16** and **17**, that were shown to be capable to bind an allosteric region rather than the catalytic site of the target enzyme, as indicated by kinetic and in silico docking studies (see below).

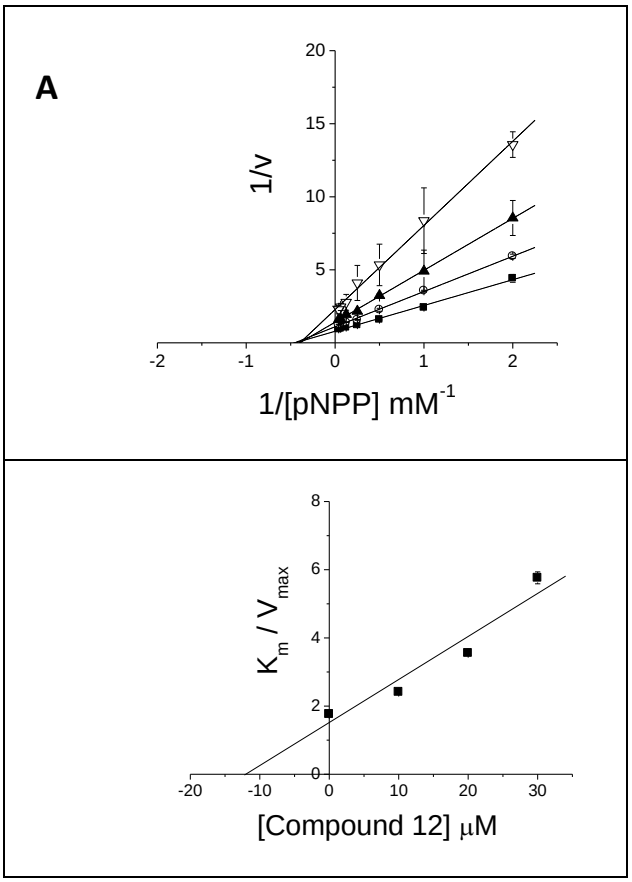

Figure 3. Kinetic analysis of compounds **12** as PTP1B inhibitor. **A)** Double reciprocal plots; the concentrations of compound **12** are: ■, 0 μM, ○, 10 μM, ▲, 20 μM, ▽, 30 μM. Data reported in the figures represent the mean values ± S.E.M. (n = 3). **B)** Secondary plots: Km/Vmax versus inhibitor concentration.

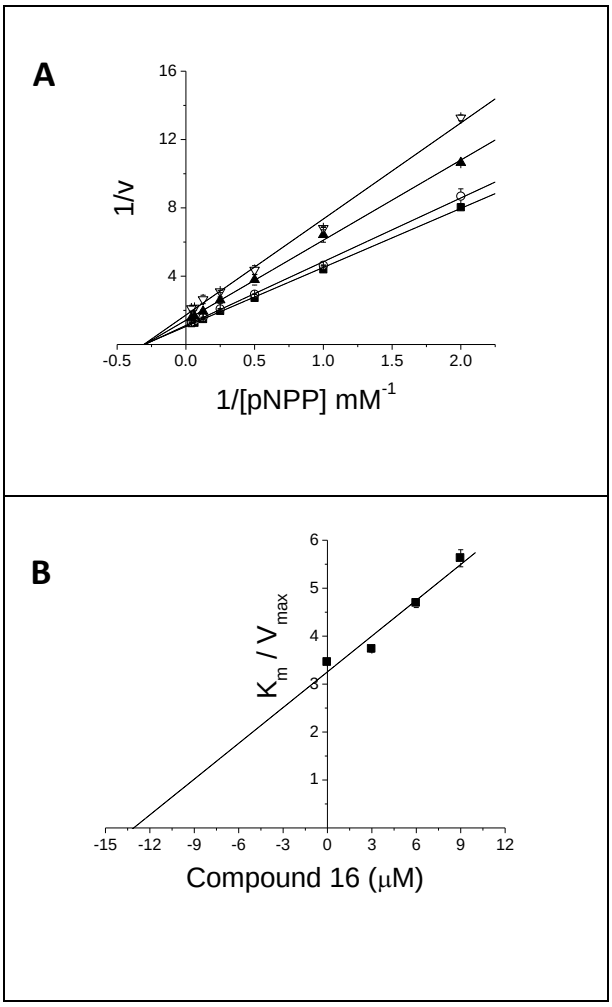

Figure 4. Kinetic analysis of compound **16** as PTP1B inhibitor. **A)** Double reciprocal plots of compound **16**; the concentrations of compound **16** are: ■, 0 μM, ○, 3 μM, ▲, 6 μM, ▽, 9 μM. Data reported in the figures represent the mean values ± S.E.M. (n = 3). **B)** Secondary plots: Km/Vmax versus inhibitor concentration.

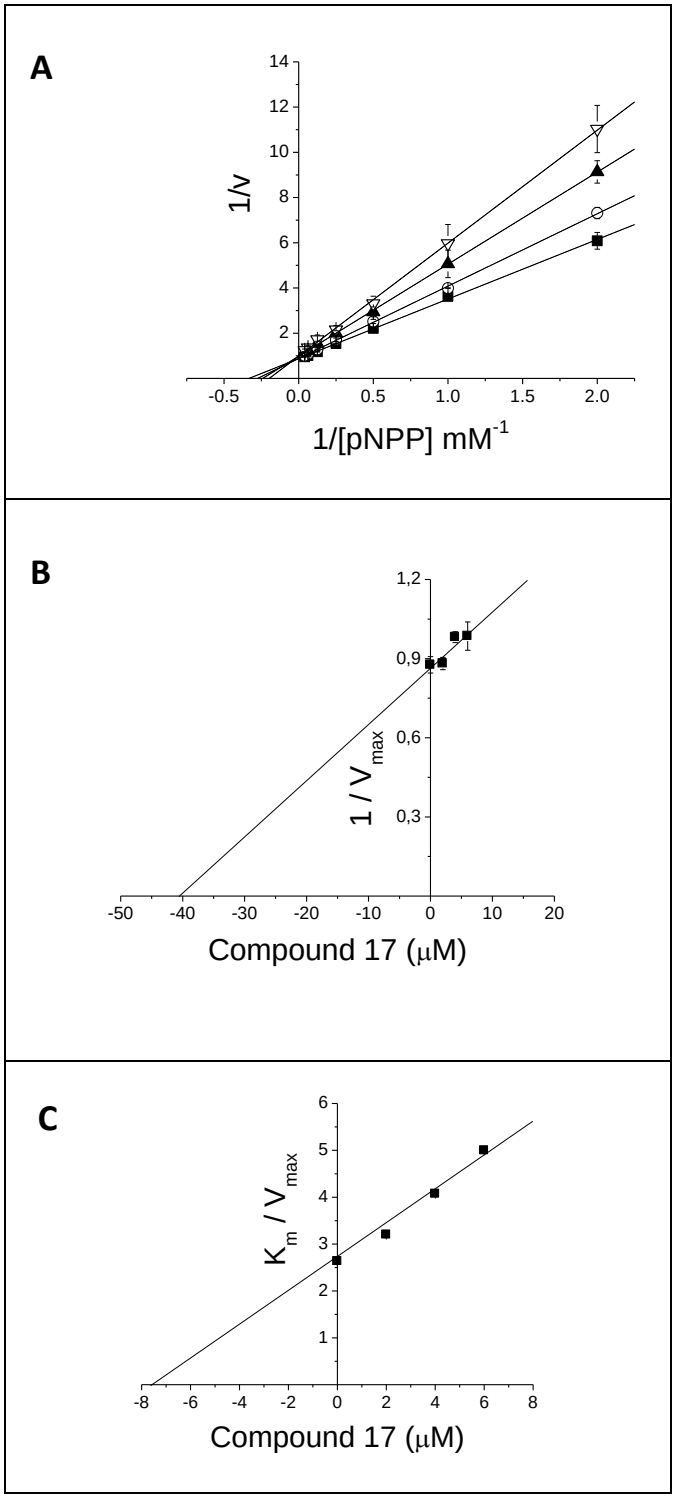

Figure 5. Kinetic analysis of compounds **17** as PTP1B inhibitor. **A)** Double reciprocal plots of compound **17**; the concentrations of compound **17** are: ■, 0 μM, ○, 2 μM, ▲, 4 μM, ▽, 6 μM. Data reported in the figures represent the mean values ± S.E.M. (n = 3). **B)** and **C)** Secondary plots: 1/Vmax, and Km/Vmax versus inhibitor concentration, respectively.

Docking studies were performed with compounds **12** and **16** in order to discover interaction features which could be useful to achieve simultaneous inhibition of both AR and PTP1B through binding to a region other than the catalytic site of the target enzymes.

The selected compounds were docked to the whole protein surface of PTP1B. In analogy to previously published 4-thiazolidinone PTP1B inhibitors,[36] compounds **12** and **16** were shown to be able to fit a site connected to the catalytic loop via a β-strand (Figure 6). Figure 7 depicts the selected pose of compound **16** bound to this allosteric site. The terminal aromatic moiety of compound **16** was found to be anchored in the lipophilic pocket of the allosteric region surrounded by residues Pro206, Arg79 and Ser80. The *meta* position of the phenylethoxy moiety allows the carboxylic group of the ligand to stretch out towards Arg105, Arg169 and Lys103, which are distal to the PTP1B catalytic site, enabling several ionic and hydrogen bonding contacts (Figure 7).

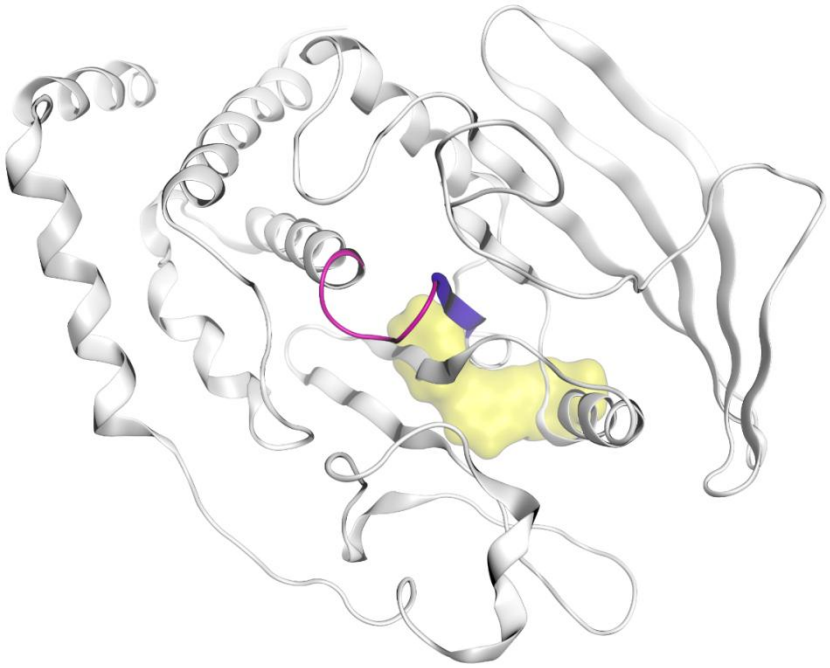

Figure 6. Representation of the second PTP1B binding site (yellow ligand shape) distal to the catalytic cavity (catalytic loop in pink), but directly connected to it by a single beta strand (violet).

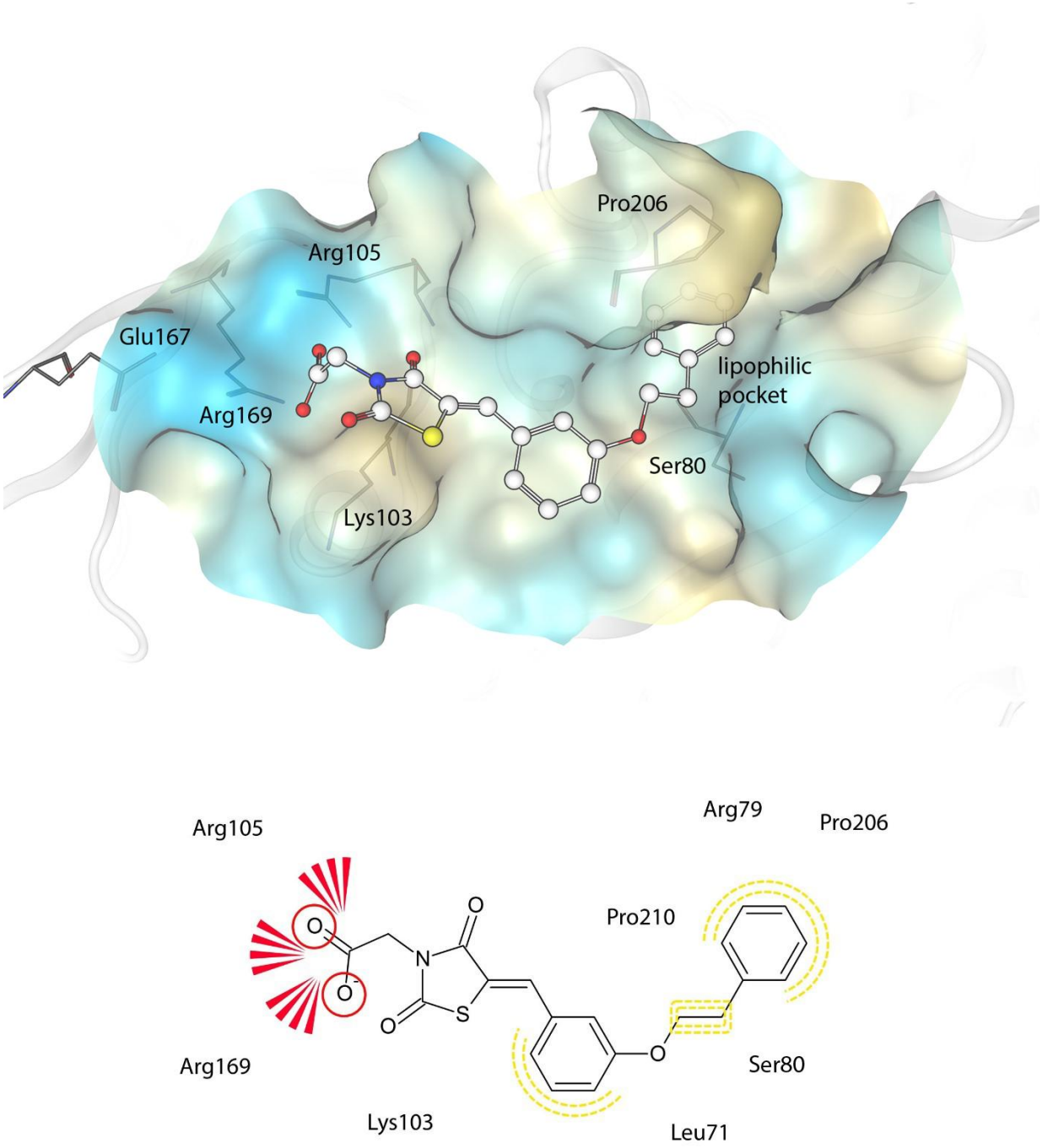

Figure 7. Selected pose of compound **16** bound to a non-catalytic binding pocket of PTP1B. *Top*: 3D depiction with protein surface coloured by hydrophilicity(cyan)/lipophilicity(yellow); inhibitor in white ball-and-stick depiction. *Bottom*: 2D depiction with protein-ligand interaction features: red circles, hydrogen bond acceptor; red stars, negative ionic interaction; yellow, hydrophobic interaction.

Protein-ligand docking of compounds **12** and **16** was performed to the AR-idose complex, since kinetic studies revealed that both compounds behave as uncompetitive AR inhibitors. So far no allosteric sites have been published for AR; however some crystal structures derived with different soaking conditions and ligand concentrations resulted in complexes with several ligands on top of each other filling the pocket connected to the catalytic site (2FZB).[40] Since no crystal structure of AR was available with idose or the corresponding alcohol, a crystal structure of AR with glyceraldehyde (3V36)[41] was modified by inserting idose instead of the former substrate.

Consistent poses were found for both compounds **12** and **16** (Figure 8). Both molecules are located in the outer part of the catalytic pocket on top of the substrate idose, which is bound to the catalytic site. The 2-phenylethoxy moiety is oriented towards idose and the catalytic residues, by filling a hydrophobic pocket above them with the possibility of hydrophobic interactions to Trp20 as well as Phe122, Trp79 and Val47. The hydrophilic part of the molecules is pointed towards the solvent with ionic and hydrogen bonding interactions of the carboxylic group with Lys221 and Arg217. The 4-carbonyl group of the thiazolidinone core shows hydrogen bonding interactions with the backbone of Ala299. The carbonyl (or thiocarbonyl) group in position 2 is faced towards the solvent, but surrounded by lipophilic sidechains of the protein, especially of Leu301. The described environment leads to a better fit of the bulkier 2-thioxo-4-thiazolidinone **12** compared to 2,4-thiazolidindione **16**, in agreement with the higher AR inhibitory potency of compound **12** compared to compound **16**. Leu301 also interacts with the adjacent 5-benzylidene ring of the ligands. This phenyl ring is also close to Trp219 with a feasible conformation that allows not only hydrophobic but also π-stacking interactions. Additionally, the bridging ether oxygen of the ligands could interact with Ser302 by means of weak hydrogen bonding interactions.

The described ligand binding poses are possible only for derivatives with *meta*-substituted 5-benzyidene ring, since they require a bent ligand arrangement in order to simultaneously fit the hydrophobic pocket above the substrate and establish ionic and hydrogen bonding interactions to Lys221 and Arg217. For an optimal fit of the hydrophobic phenyl moiety to the hydrophobic cavity a certain length of the spacer between the phenyl rings is also required and a spacer length between three and four atoms appeared to be the most suitable for this purpose.

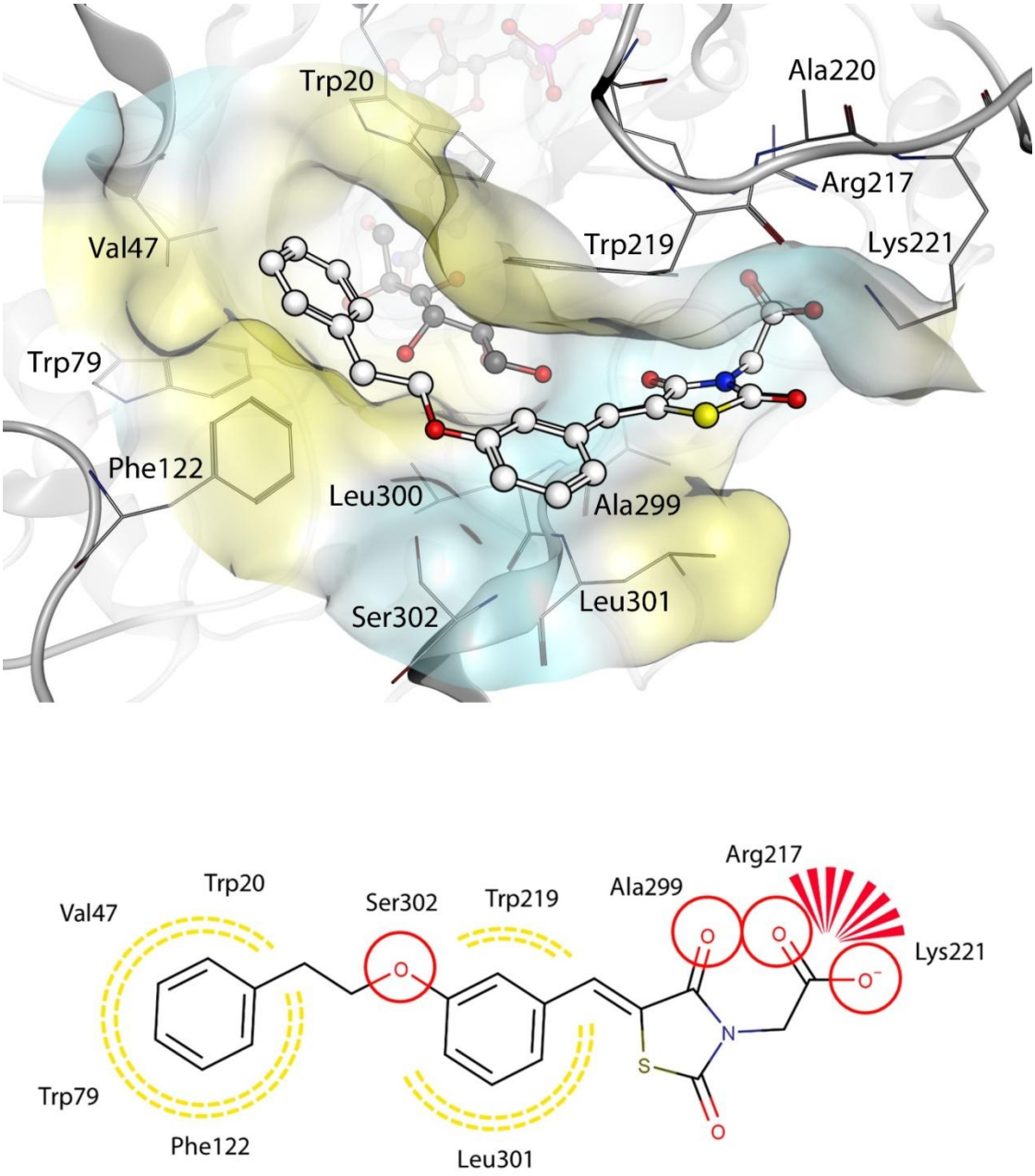

Figure 8. Selected pose of compound **16** bound to the AR-idose complex. *Top*: 3D depiction with protein surface coloured by hydrophilicity(cyan)/lipophilicity(yellow); inhibitor in white, substrate in dark grey. *Bottom*: 2D depiction with protein-ligand interaction features: red circles, hydrogen bond acceptor; red stars, negative ionic interaction; yellow, hydrophobic interaction.

Based on the conducted docking and SAR investigations, a main goal of this study was that several ligand features were identified as important for simultaneous inhibiting both AR and PTP1B enzymes through binding to non-catalytic regions. Firstly, both allosteric binding sites require a bent ligand arrangement that is enabled by the 3-(2-phenylethoxy)benzylidene moiety (in compounds **12** and **16**) relative to the thiazolidinone core. Secondly, the central part of the ligand, characterized in these compounds by the 5-benzylidene ring, needs to be relatively lipophilic, but even more the distal part of the ligand, which is buried in the lipophilic pocket in PTP1B and positioned in a lipophilic cleft on top of the substrate in AR. Furthermore, our studies revealed that this terminal portion shows optimal fit to both binding sites of the two target enzymes for a distance of approximately 8 Å to C5 of the central phenyl ring of the ligand. Additionally, to ensure an effective binding, an acidic moiety is highly beneficial, which should be able to bent out of the plane defined by the rest of the binding site to reach basic amino acid residues present in both allosteric binding sites.

Our findings highlight that the chance of exploiting allosteric regions to effectively inhibit both human AR and PTP1B offers promising opportunities for the design of new dual inhibitors of these target enzymes.

Declarations of interest

None.

Acnowledgements

This work was supported by University of Messina, University of Florence and University of Pisa and by a fund to P.P. from Italian Ministry of University and Research (Miur - Finanziamento annuale individuale delle attività base di ricerca 2018).

The Authors thank Prof. Umberto Mura for critical reading of the enzymological section.

References

[1] http://www.who.int/diabetes

[2] Guariguata L, Whiting DR, Hambleton I, Beagley J, Linnenkamp U, Shaw JE. Global estimates of diabetes prevalence for 2013 and projections for 2035. *Diabetes Res. Clin. Pract.* 2014; 103: 137-149.

[3] Brownlee M. Biochemistry and molecular cell biology of diabetic complications. *Nature* 2001; 414: 813-820.

[4] Csermely P, Agoston V, Pongor S. The efficiency of multi-target drugs: the network approach might help drug design. *Trends Pharmacol. Sci.* 2005; 26: 178-182.

[5] Morphy R, Rankovic Z. Designed Multiple Ligands. An Emerging Drug Discovery Paradigm. *J. Med. Chem.* 2005; 48: 6523-6543.

[6] Hopkins A. Network pharmacology: the next paradigm in drug discovery. *Nature Chem. Biol.* 2008; 4: 682-690.

[7] Gattrell W, Johnstone C, Patel S, Sambrook Smith C, Scheel A, Schindler M. Designed multiple ligands in metabolic disease research: from concept to platform. *Drug Discov. Today* 2013; 18: 692-696.

[8] Costantino L, Barlocco D. Designing approaches to multitarget drugs. In: Handler H, Buschmann H, eds. *Drug selectivity: an evolving concept in medicinal chemistry*. Wiley-VCH, Weinheim, 2018.

[9] Zabolotny JM, Bence-Hanulec KK, Stricker-Krongrad A, Haj F, Wang Y, Minokoshi Y, Kim YB, Elmquist JK, Tartaglia LA, Kahn BB, Neel BG. PTP1B regulates leptin signal transduction in vivo. *Dev. Cell* 2002; 2: 489-495.

[10] Cheng A, Uetani N, Simoncic PD, Chaubey VP, Lee-Loy A, McGlade CJ, Kennedy BP, Tremblay ML. Attenuation of leptin action and regulation of obesity by protein tyrosine phosphatase 1B. *Dev. Cell* 2002; 2: 497-503.

[11] Elchebly M, Payette P, Michaliszyn E, Cromlish W, Collins S, Loy AL, Normandin D, Cheng A, Himms-Hagen J, Chan CC, Ramachandran C, Gresser MJ, Tremblay ML, Kennedy BP. Increased insulin sensitivity and obesity resistance in mice lacking the protein tyrosine phosphatase-1B gene. *Science* 1999; 283: 1544-1548.

[12] Klaman LD, Boss O, Peroni OD, Kim JK, Martino JL, Zabolotny JM, Moghal N, Lubkin M, Kim YB, Sharpe AH, Stricker-Krongrad A, Shulman GI, Neel BG, Kahn BB. Increased energy expenditure, decreased adiposity, and tissue-specific insulin sensitivity in protein-tyrosine phosphatase 1B–deficient mice. *Mol. Cell. Biol.* 2000; 20: 5479-5489.

[13] Di Paola R, Frittitta L, Miscio G, Bozzali M, Baratta R, Centra M, Spampinato D, Santagati MG, Ercolino T, Cisternino C, Soccio T, Mastroianno S, Tassi V, Almgren P,

Pizzuti A, Vigneri R, Trischitta V. A variation in 3' UTR of hPTP1B increases specific gene expression and associates with insulin resistance. *Am. J. Hum. Genet.* 2002; 70: 806-812.

[14] Bence KK, Delibegovic M, Xue B, Gorgun CZ, Hotamisligil GS, Neel BG, Kahn BB. Neuronal PTP1B regulates body weight, adiposity and leptin action. *Nat. Med.* 2006; 12: 917-924.

[15] Zhang ZY, Dodd GT, Tiganis T. Protein tyrosine phosphatases in hypothalamic insulin and leptin signalling. *Trends Pharmacol. Sci.* 2015; 36: 661-674.

[16] Srivastava SK, Ramana KV, Bhatnagar A. Role of aldose reductase and oxidative damage in diabetes and the consequent potential for therapeutic options. *Endocr. Rev.* 2005; 26: 380-392.

[17] Maccari R, Ottanà R. Targeting aldose reductase for the treatment of diabetes complications and inflammatory diseases: new insights and future directions. *J. Med. Chem.* 2015; 58: 2047-2067.

[18] Hubatsch I, Ridderström M, Mannervik B. Human glutathione transferase A4-4: an alpha class enzyme with high catalytic efficiency in the conjugation of 4-hydroxynonenal and other genotoxic products of lipid peroxidation. *Biochem. J.* 1998; 330: 175-179.

[19] Frohnert BI, Long EK, Hahn WS, Bernlohr DA. Glutathionylated lipid aldehydes are products of adipocyte oxidative stress and activators of macrophage inflammation. *Diabetes* 2014; 63: 89-100.

[20] Ramana KV, Srivastava SK. Aldose reductase: a novel therapeutic target for inflammatory pathologies. *Int. J. Biochem. Cell Biol.* 2010; 42: 17-20.

[21] Chatzopoulou M, Pegklidou K, Papastavrou N, Demopoulos VJ. Development of aldose reductase inhibitors for the treatment of inflammatory disorders. *Expert Opin. Drug Discov.* 2013; 8: 1365-1380.

[22] Vyas B, Silakari O, Kaur M, Singh B. Integrated pharmacophore and docking-based designing of dual inhibitors of aldose reductase (ALR2) and protein tyrosine phosphatase (PTP1B) as novel therapeutics for insulin-resistant diabetes and its complications. *J. Chemometrics* 2015; 29: 109-125.

[23] Bruno G, Costantino L, Curinga C, Maccari R, Monforte F, Nicolò F, Ottanà R, Vigorita MG. Synthesis and aldose reductase inhibitory activity of 5-arylidene-2,4-thiazolidinediones. *Bioorg. Med. Chem.* 2002; 10: 1077-1084.

[24] Maccari R, Ottanà R, Curinga C, Vigorita MG, Rakowitz D, Steindl T, Langer T. Structure–activity relationships and molecular modelling of 5-arylidene-2,4-

thiazolidinediones active as aldose reductase inhibitors. *Bioorg. Med. Chem.* 2005; 13: 2809-2823.

[25] Maccari R, Ottanà R, Ciurleo R, Vigorita MG, Rakowitz D, Steindl T, Langer T. Evaluation of in vitro aldose redutase inhibitory activity of 5-arylidene-2,4-thiazolidinediones. *Bioorg. Med. Chem. Lett.* 2007; 17: 3886-3893.

[26] Maccari R, Ottanà R, Ciurleo R, Rakowitz D, Matuszczak B, Laggner C, Langer T. Synthesis, induced-fit docking investigations, and in vitro aldose reductase inhibitory activity of non-carboxylic acid containing 2,4-thiazolidinedione derivatives. *Bioorg. Med. Chem.* 2008; 16: 5840-5852.

[27] Maccari R, Ciurleo R, Giglio M, Cappiello M, Moschini R, Del Corso A, Mura U, Ottanà R. Identification of new non-carboxylic acid containing inhibitors of aldose reductase. *Bioorg. Med. Chem.* 2010; 18: 4049-4055.

[28] Ottanà R, Maccari R, Giglio M, Del Corso A, Cappiello M, Mura U, Cosconati S, Marinelli L, Novellino E, Sartini S, La Motta C, Da Settimo F. Identification of 5-arylidene-4-thiazolidinone derivatives endowed with dual activity as aldose reductase inhibitors and antioxidant agents for the treatment of diabetic complications. *Eur. J. Med. Chem.* 2011; 46: 2797-2806.

[29] Maccari R, Del Corso A, Giglio M, Moschini R, Mura U, Ottanà R. In vitro evaluation of 5-arylidene-2-thioxo-4-thiazolidinones active as aldose reductase inhibitors. *Bioorg. Med. Chem. Lett.* 2011; 21: 200-203.

[30] Maccari R, Vitale RM, Ottanà R, Rocchiccioli M, Marrazzo A, Cardile V, Graziano ACE, Amodeo P, Mura U, Del Corso A. Structure-activity relationships and molecular modelling of new 5-Arylidene-4-thiazolidinone derivatives as aldose reductase inhibitors and potential anti-inflammatory agents. *Eur. J. Med. Chem.* 2014; 81: 1-14.

[31] Maccari R, Paoli P, Ottanà R, Jacomelli M, Ciurleo R, Manao G, Steindl T, Langer T, Vigorita MG, Camici G. 5-Arylidene-2,4-thiazolidinediones as inhibitors of protein tyrosine phosphatases. *Bioorg. Med. Chem.* 2007; 15: 5137-5149.

[32] Ottanà R, Maccari R, Ciurleo R, Paoli P, Jacomelli M, Manao G, Camici G, Laggner C, Langer T. 5-Arylidene-2-phenylimino-4-thiazolidinones as PTP1B and LMW-PTP inhibitors. *Bioorg. Med. Chem.* 2009; 17: 1928-1937.

[33] Maccari R, Ottanà R, Ciurleo R, Paoli P, Manao G, Camici G, Laggner C, Langer T. Structure-based optimization of benzoic acids as inhibitors of protein tyrosine phosphatase 1B and low molecular weight protein tyrosine phosphatase. *ChemMedChem* 2009; 4: 957-962.

[34] Ottanà R, Maccari R, Amuso S, Wolber G, Schuster D, Herdlinger S, Manao G, Camici G, Paoli P. New 4-[(5-Arylidene-2-arylimino-4-oxo-3-thiazolidinyl)methyl]benzoic acids active as protein tyrosine phosphatase inhibitors endowed with insulinomimetic effect on mouse C2C12 skeletal muscle cells. *Eur. J. Med. Chem.* 2012; 50: 332-343.

[35] Ottanà R, Maccari R, Mortier J, Caselli A, Amuso S, Camici G, Rotondo A, Wolber G, Paoli P. Synthesis, biological activity and structure-activity relationships of new benzoic acid-based protein tyrosine phosphatase inhibitors endowed with insulinomimetic effects in mouse C2C12 skeletal muscle cells. *Eur. J. Med. Chem.* 2014; 71: 112-127.

[36] Ottanà R, Paoli P, Naß A, Lori G, Cardile V, Adornato I, Rotondo A, Graziano ACE, Wolber G, Maccari R. Discovery of 4-[(5-arylidene-4-oxothiazolidin-3-yl)methyl]benzoic acid derivatives active as novel potent allosteric inhibitors of protein tyrosine phosphatase 1B: In silico studies and in vitro evaluation as insulinomimetic and anti-inflammatory agents. *Eur. J. Med. Chem.* 2017; 127: 840-858.

[37] Ottanà R, Maccari R, Barreca ML, Bruno G, Rotondo A, Rossi A, Chiricosta G, Di Paola R, Sautebin L, Cuzzocrea S, Vigorita MG. 5-Arylidene-2-imino-4-thiazolidinones: design and synthesis of novel antiinflammatory agents. *Bioorg. Med. Chem.* 2005; 13: 4243-4252.

[38] Balestri F, Cappiello M, Moschini R, Rotondo R, Buggiani I, Pelosi P, Mura U, Del Corso A. L-Idose: an attractive substrate alternative to D-glucose for measuring aldose reductase activity. *Biophys. Res. Commun.* 2015; 456: 891-895.

[39] Balestri F, Cappiello M, Moschini R, Rotondo R, Abate A, Del Corso A, Mura U. Modulation of aldose reductase activity by aldose hemiacetals. *Biochim. Biophys. Acta* 2015; 1850: 2329-2339.

[40] Steuber H, Zentgraf M, Gerlach C, Sotriffer CA, Heine A, Klebe G. Expect the unexpected or caveat for drug designers: multiple structure determinations using aldose reductase crystals treated under varying soaking and co-crystallisation conditions. *J. Mol. Biol.* 2006; 363: 174-187.

[41] Zheng X, Zhang L, Chen W, Chen Y, Xie W, Hu X. Partial inhibition of aldose reductase by nitazoxanide and its molecular basis. *ChemMedChem* 2012; 7: 1921-1923.

An investigation on 4-thiazolidinone derivatives as dual inhibitors of aldose reductase and protein tyrosine phosphatase 1B, in the search for potential agents for the treatment of type 2 diabetes mellitus and its complications

Rosanna Maccari,[a]* Antonella Del Corso,[b] Paolo Paoli,[c] Ilenia Adornato,[a] Giulia Lori,[c] Francesco Balestri,[b] Mario Cappiello,[b] Alexandra Naß,[d] Gerhard Wolber,[d] Rosaria Ottanà[a]

[a] *Department of Chemical, Biological, Pharmaceutical and Environmental Sciences, University of Messina, Polo Universitario Annunziata, Viale SS. Annunziata, 98168 Messina, Italy*

[b] *Department of Biology, Biochemistry Unit, University of Pisa, Via S. Zeno, 51, 56123 Pisa, Italy*

[c] *Department of Scienze Biomediche Sperimentali e Cliniche, Sezione di Scienze Biochimiche, University of Firenze, Viale Morgagni 50, 50134 Firenze, Italy*

[d] *Institute of Pharmacy, Computer-Aided Molecular Design, Freie Universitaet Berlin, Koenigin-Luisestr. 2+4, 14195 Berlin, Germany*

* Corresponding author – email: rmaccari@unime.it

SUPPLEMENTARY DATA

Materials and Methods

1. Chemistry

Melting points were recorded on a Kofler hot-stage apparatus and are uncorrected. TLC controls were carried out on precoated silica gel plates (F 254 Merck). Combustion analyses (C, H, N),determined by means of a C. Erba mod. 1106 elem. Analyzer, were within ± 0.4% of the theoretical values. ^{1}H and ^{13}C NMR spectra were achieved by a Bruker Avance 300 MHz and a Varian 500 MHz spectrometers controlled by Linux workstations running TOPSPIN and vNMRj software packages respectively. All data were analyzed on a PC by the Mestrenova software package (version 6.0.2, Mestrelab research S.L.). All the spectra were phased, baseline was corrected where necessary and DMSO-d_6

signals were used as reference for both ^{1}H and ^{13}C spectra. Unless stated otherwise, all materials were obtained from commercial suppliers and used without further purification. For the synthesis of compound **10**, *trans*-cinnamaldehyde (Sigma-Aldrich) was used. The purity of synthetic compounds was established as ≥ 95% by combustion analysis.

Compounds **1**-**9** were synthesised according to previously reported procedures (see Refs. 29, 30 of the article).

*1.1 General procedure for the synthesis of (5-arylidene-4-oxo-2-thioxothiazolidin-3-yl)acetic acids **10-13***

A mixture of (4-oxo-2-thioxothiazolidin-3-yl)acetic acid (1.15 g, 6 mmol), appropriate aldehyde (6 mmol), sodium acetate (3.69 g, 45 mmol) and glacial acetic acid (30 ml) was refluxed for 4-5 hrs. The reaction mixture was poured into H_2O and filtered off. The crude solid was recrystallized from methanol to provide pure compounds **10**-**13**.

*1.1.1 [4-Oxo-5-(3-phenyl-2-propen-1-ylidene)-2-thioxothiazolidin-3-yl]acetic acid **10***

Yield 23%; mp 262-265 °C; ^{1}H NMR (DMSO-d_6): δ 4.50 (s, 2H, NCH_2); 7.10 (dd J=15.0 Hz and J=11.4 Hz, 1H, =CH); 7.38-7.43 (m, 4H, arom and =CH); 7.55 (d J=11.4 Hz, 1H, =CH); 7.70-7.73 (m, 2H, arom). ^{13}C NMR (DMSO-d_6): δ 47.6, 119.0, 124.9, 127.5, 128.5, 128.6, 135.4, 136.2, 138.2, 167.6, 169.0, 194.7. Anal. ($C_{14}H_{11}NO_3S_2$) calcd: C 55.07; H 3.63; N 4.59, found: C 55.28; H 3.71; N 4.35.

*1.1.2 (4-Oxo-5-{[4-(2-phenylethoxy)phenyl]methylidene}-2-thioxothiazolidin-3-yl)acetic acid **11***

Yield 42%; mp 237-240 °C; ^{1}H NMR (DMSO-d_6): δ 3.06 (t J=6.6 Hz, 2H, $PhCH_2$), 4.30 (t J=6.6 Hz, 2H, CH_2), 4.52 (s, 2H, NCH_2), 7.13 (m, 2H, arom), 7.28-7.33 (m, 5H, arom), 7.62 (m, 2H, arom), 7.78 (s, 1H, CH methylidene). ^{13}C NMR (DMSO-d_6): δ 35.5, 47.4, 69.3, 114.3, 116.5, 125.9, 126.4, 127.2, 129.2, 129.8, 138.9, 143.3, 161.5, 167.5, 167.9, 193.9. Anal. ($C_{20}H_{17}NO_4S_2$) calcd: C 60.13; H 4.29; N 3.51, found: C 59.97; H 4.47; N 3.39.

1.1.3 (4-Oxo-5-{[3-(2-phenylethoxy)phenyl]methylidene}-2-thioxothiazolidin-3-yl)acetic acid

12

Yield 24%; mp 172-175 °C; ^{1}H NMR (DMSO-d_6): δ 3.06 (t J=6.6 Hz, 2H, $PhCH_2$), 4.26 (t J=6.6 Hz, 2H, OCH_2), 4.73 (s, 2H, NCH_2), 7.11 (m, 1H, arom), 7.23-7.29 (m, 3H, arom), 7.32-7.35 (m, 4H, arom), 7.50 (m, 1H, arom), 7.86 (s, 1H, CH methylidene). ^{13}C NMR (DMSO-d6): δ 35.1, 45.4, 68.8, 116.7, 118.5, 122.5, 122.9, 126.8, 128.6, 129.7, 131.0, 134.4, 134.9, 138.6, 159.2, 166.8, 167.7, 193.7. Anal. ($C_{20}H_{17}NO_4S_2$) calcd: C 60.13; H 4.29; N 3.51, found: C 60.26; H 4.45; N 3.67.

1.1.4 {5-[(4-Benzyloxy-3-methoxyphenyl)methylidene]-4-oxo-2-thioxothiazolidin-3-yl}acetic acid ***13***

Yield 73%; mp 277-280 °C; ^{1}H NMR (DMSO-d_6): δ 3.84 (s, 3H, OCH_3), 4.49 (s, 2H, NCH_2), 5.19 (s, 2H, OCH_2), 7.24-7.26 (m, 3H, arom), 7.34-7.46 (m, 5H, arom), 7.78 (s, 1H, CH methylidene). ^{13}C NMR (DMSO-d_6): δ 48.6, 56.1, 71.6, 110.5, 114.8, 116.0, 123.0, 126.4, 128.4, 128.5, 128.8, 136.7, 143.3, 144.9, 149.7, 166.4, 169.7, 194.0. Anal. ($C_{20}H_{17}NO_5S_2$) calcd: C 57.82; H 4.12; N 3.37, found: C 58.03; H 4.27; N 3.18.

1.2 General procedure for the synthesis of (5-arylidene-2,4-dioxothiazolidin-3-yl)acetic acids ***14-16***

A mixture of 2,4-thiazolidinedione (1.76 g, 15 mmol), appropriate aldehyde (10 mmol) and piperidine (1.02 g, 12 mmol) in ethanol was refluxed for 24 hrs. The crude mixture was poured into H_2O acidified with AcOH (pH 3-4) to give a crude solid which was recrystallized from methanol to provide the corresponding pure 5-arylidene-2,4-thiazolidinedione. A mixture of 5-arylidene-2,4-thiazolidinedione (10 mmol), methyl bromoacetic acid (2.78 g, 20 mmol) and potassium carbonate (5.53 g, 40 mmol) in anhydrous acetone (120 ml) was refluxed for 24 hrs. The solvent was evaporated under reduced pressure. The solid residue was poured into H_2O, acidified with HCl 6N (pH 3) and stirred until CO_2 disappearance. The solid was filtered off, washed with H_2O and recrystallized from methanol providing pure compounds **14**-**16**.

1.2.1 (5-{[4-(2-Phenylethoxy)pheny]methylidene}-2,4-dioxothiazolidin-3-yl)acetic acid ***14***

Yield 47%; mp 176-178 °C; ^{1}H NMR (DMSO-d_6): δ 3.05 (t J=6.9 Hz, 2H, $PhCH_2$), 4.28 (t J=6.9 Hz, 2H, OCH_2), 4.36 (s, 2H, NCH_2), 7.13 (m, 2H, arom), 7.15-7.32 (m, 5H, arom), 7.61 (m, 2H, arom), 7.93 (s, 1H, CH methylidene). ^{13}C NMR (DMSO-d_6): δ 35.0, 42.6, 68.7, 115.9, 117.8, 125.8, 126.9, 128.8, 129.4, 132.8, 134.3, 138.7, 160.9, 165.5, 167.6, 168.6. Anal. ($C_{20}H_{17}NO_5S$) calcd: C 62.65; H 4.47; N 3.65, found: C 62.54; H 4.58; N 3.43.

1.2.2 {5-[(4-Benzyloxy-3-methoxyphenyl)methylidene]-2,4-dioxothiazolidin-3-yl}acetic acid ***15***

Yield 74%; mp 243-246 °C; ^{1}H NMR (DMSO-d_6): δ 3.81 (s, 3H, OCH_3), 4.35 (s, 2H, NCH_2), 5.16 (s, 2H, OCH_2), 7.21-7.46 (m, 6H, arom), 7.92 (s, 1H, CH methylidene). ^{13}C NMR (DMSO-d_6): δ 42.8, 55.9, 70.5, 113.8, 114.0, 118.5, 124.4, 126.0, 128.1, 128.5, 128.9, 134.7, 136.9, 149.6, 150.7, 165.6, 167.5, 168.5. Anal. ($C_{20}H_{17}NO_6S$) calcd: C 60.14; H 4.29; N 3.51, found: C 60.31; H 4.42; N 3.39.

1.2.3 (5-{[3-(2-Phenylethoxy)phenyl]methylidene}-2,4-dioxothiazolidin-3-yl)acetic acid ***16***

Yield 34%; mp 160 °C (dec.); ^{1}H NMR (DMSO-d_6): δ 3.04 (t J=6.6 Hz, 2H, $PhCH_2$), 4.15 (s, 2H, NCH_2), 4.23 (t J=6.6 Hz, 2H, OCH_2), 7.06 (m, 1H, arom), 7.19-7.34 (m, 7H, arom), 7.43 (m, 1H, arom), 7.90 (s, 1H, CH methylidene). ^{13}C NMR (DMSO-d_6): δ 35.3, 44.2, 68.9, 116.4, 117.6, 122.0, 122.3, 126.8, 129.0, 129.6, 130.9, 133.7, 134.8, 138.8, 159.3, 165.7, 167.3, 168.1. Anal. ($C_{20}H_{17}NO_5S$) calcd: C 62.65; H 4.47; N 3.65, found: C 62.39; H 4.56; N 3.48.

1.3 Synthesis of {5-[(4-Benzyloxy-3-methoxyphenyl)methylidene]-4-oxo-2-phenyliminothiazolidin-3-yl}acetic acid ***17***

A mixture of (4-oxo-2-phenyliminothiazolidin-3-yl)acetic acid (0.38 g, 1.5 mmol), which was synthesised according to a previously reported procedure (see Ref. 28 of the article), 4-benzyloxy-3-methoxybenzaldehyde (0.24 g, 1.0 mmol) and piperidine (0.21 g, 2.4 mmol) in EtOH (20 ml) was refluxed for 26 h. The reaction mixture was poured into water, acidified with glacial AcOH (pH 3-

4) and filtered off. The crude solid was recrystallized from methanol to give pure compound **17**.

Yield 19%; yellow oil; ^{1}H NMR (DMSO-d_6): δ 3.73 (s, 3H, OCH_3), 4.56 (s, 2H, NCH_2), 5.09 (s, 2H, OCH_2), 6.95-7.02 (m, 3H, arom), 7.12-7.22 (m, 3H, arom), 7.30-7.41 (m, 7H, arom), 7.74 (s, 1H, CH methylidene). ^{13}C NMR (DMSO-d_6): δ 44.5, 56.0, 69.9, 111.3, 114.5, 116.0, 122.1, 122.6, 127.5, 127.6, 128.3, 129.1, 130.3, 136.9, 145.7, 149.3, 150.0, 160.7, 166.8, 169.3. Anal. ($C_{26}H_{22}N_2O_5S$) calcd: C 65.81; H 4.67; N 5.90, found: C 66.02; H 4.79; N 5.71.

2. Docking methods

For all docking investigations, publicly available crystal structures from the Protein Data Bank[1] were selected and downloaded. Preparation of the structures for docking was performed using the software MOE (version 2015).[2] Docking studies were performed using the software GOLD.[3] 25 poses were generated per ligand and selected based on RMSD clustering of the poses. Selected ligand poses were energy minimized together with surrounding amino acids using MOE. Protein-ligand interaction pictures were derived from LigandScout[4,5] pharmacophores.

2.1 Allosteric Docking to PTP1B

For PTP1B docking crystal structure 1Q6T was chosen and preparation and protein-ligand docking was performed as described in our previous publication (see Ref. 36 of the article).

2.2 Docking to the Aldose Reductase Enzyme-Substrate Complex

Crystal structure 3V36 was chosen to build the enzyme substrate complex, since it contains a co-crystallized glyceraldehyde in the catalytic pocket. This ligand was then modified manually to idose using MOE.[2] Idose was then energy minimized inside the catalytic pocket with the MMFF94x force field. Docking was performed into the protein structure containing NADPH and idose. As binding location the volume with 12 Å radius around the outmost C-atom of idose was chosen to enforce poses close to the substrate.

3. Enzymatic assays

3.1 Expression, purification and enzymatic assay of AR

The expression and purification of human recombinant aldose reductase (AR) were performed as previously described.[6] The purified enzyme (specific activity 5.0 U/mg) was stored at -80 °C in 10 mM sodium phosphate buffer pH 7.0 containing 2 mM dithiothreitol and 30 % (w/v) glycerol. The enzyme was extensively dialyzed against 10 mM sodium phosphate buffer pH 7.0 before use. The enzymatic activity was measured spectrophotometrically at 37 °C as previously described.[7] One Unit of enzyme activity refers to the amount of enzyme that catalyzes the oxidation of 1 μmol/min of NADPH using 4.7 mM D,L-glyceraldehyde as substrate.

3.2 Inhibition studies on AR

For the determination of IC_{50} (concentration of compound required to determine a 50% inhibition of enzyme activity) values, the assay mixture (final volume 0.7 mL) contained, in 0.25 M sodium phosphate buffer pH 6.8, 2 mM L-idose, 0.11 mM NADPH, 0.38 M ammonium sulphate and 0.5 mM EDTA. Compounds **1-17**, tested as aldose reductase inhibitors were dissolved in DMSO and added to the above described assay mixture containing 8 mU of purified AR. The reaction was started by addition of the substrate. The DMSO concentration in all the assays was kept constant at 0.5% (v/v).

The IC_{50} values were determined by nonlinear regression analysis using Prism GraphPad 6.0 fitting experimental data to the following equation:

$$\frac{v_i}{v_0} = \frac{Max - Min}{1 + \left(\frac{[I]}{IC\,50}\right)^{slope}} + Min \qquad \text{(Eq. 1)}$$

In the equation v_i/v_0, represents the ration between the activity measured in the presence of the inhibitor and the activity measured in the absence of inhibitor; *Max* and *Min* represent the expected maximal and minimal value of activity and were fixed at 1 and zero, respectively. Slope, which describes the steepness of curve in the transition region, was fixed at -1. For each compound, at least five different concentrations of inhibitor in triplicate assay were analyzed.

Compounds **12** and **16** were further analyzed and both their model of action and inhibition constants were determined. In this case, the enzymatic assay contained 7 mU of AR (67 nM, calculated on the basis of a molecular weight of

34KDa), different concentrations of L-idose, ranging from 2 to 16 mM, and different concentrations of the inhibitors. Since the IC_{50} values resulted of the same order of magnitude as the enzyme concentration in the assay, compounds **12** and **16** were treated as "tight binding inhibitors". Thus the residual activity measurements obtained at each substrate concentration were fitted by nonlinear regression analysis to Morrison equation.[8]

$$v_i = 1 - \frac{\left([E_T] + [I] + K_i^{app}\right) - \sqrt{\left([E_T] + [I] + K_i^{app}\right)^2 - 4[E_T][I]}}{2[E_T]} \quad \text{(Eq. 2)}$$

for K_i^{app} evaluation. In order to obtain the inhibition constants K_i (dissociation constant of the EI complex) and $K_i^{'}$, (dissociation constant of the EIS complex), the K_i^{app} values were plotted against substrate concentration, and fitted by nonlinear regression analysis to the equation

$$K_i^{app} = ([S] + K_M) / (K_M / K_i + [S] / K_i^{'}) \quad \text{(Eq.3)}$$

relative to a general case of tight binding non-competitive inhibition model. The used K_M value for L-idose, was 3.8 mM.[6]

In order to evaluate the reversibility of the inhibitory action, 8 mU of AR were assayed in the presence of 0.25 μM or 2 μM of either compound **12** or **16**, respectively. In these conditions less than 5% of the enzyme activity was measured in the presence of 2 mM L-idose as substrate. The mixture was then extensively dialysed on Amicon ultrafiltation membrane (Cut off 10 KDa) against 10 mM sodium phosphate buffer, pH7.0. After dialysis the recovery of enzyme activity was measured as above.

3.3 Expression and purification of recombinant PTP1B

The sequence of full-length human protein tyrosine phosphatase 1B (PTP1B) was cloned in the pGEX-2T bacterial expression vector to obtain GST-PTP1B fusion protein. Fusion protein was purified by single step affinity chromatography by using a column loaded with glutathione-Sepharose resin. Fractions containing fusion protein were collected, concentrated up to 5 ml volume. Then, the solution containing purified fusion proteins was incubated

with thrombin for 3 h at 37 °C. Finally, PTP1B, GST and thrombin were separated by using a gel filtration column loaded with Superdex G-75 resin. The purity of protein preparations was checked by SDS–PAGE. Purified PTP1B (specific activity 80 U/mg) was stored at -80°C.

3.4 Inhibition studies on PTP1B

For the determination of IC_{50} values, the assay mixture (final volume 1 mL) contained, in 75 mM β,β-dimethylglutarate buffer pH 7, 1 mM EDTA and 2.5 mM pNPP (CAS 4264-83-9) as substrate. After incubation at 37°C, the reaction was stopped by adding 4 ml of 0.1 M KOH solution. The amount of p-nitrophenolate released was determined reading the absorbance of samples at 400 nm (ε_{mM} 18 cm^{-1}). Compounds **1-17**, tested as PTP1B inhibitors were dissolved in DMSO and added to the above described assay mixture containing 0.4 U of purified PTP1B. The DMSO concentration in all the assays was kept constant at 5 % (v/v). The IC_{50} values were calculated by measuring initial pNPP hydrolysis rate in the presence of increasing inhibitors concentration. For these tests, the substrate concentration was fixed at 2.5 mM, a value corresponding to K_M of enzyme. The IC_{50} value was determined fitting experimental data by using equation 1 (see paragraph 3.2).

To evaluate whether molecules behave as reversible or irreversible inhibitors, a dilution test was carried out. Briefly, 3.6 units of the enzyme were incubated at 37°C for 60 minutes with the inhibitor present at a concentration able to reduce the activity of 95%. An aliquot of the mixture was then diluted 400 folds in the assay buffer to evaluate the eventual recovery of enzyme activity, with respect to an enzyme aliquot incubated in the same conditions in the absence of the inhibitor.

The action mechanism of inhibitors was determined by studying the dependence of K_M and V_{max} on the inhibitor concentration. Both parameters were calculated measuring the initial hydrolysis rates in the presence of increasing substrate concentrations and fitting data using the Michaelis-Menten equation. Finally, the inhibition constant (Ki) was determined using the appropriate equation, depending from the inhibition mechanism proposed. All tests were carried out in triplicate.

References

[1] Berman HM, Westbrook J, Feng Z, Gilliland G, Bhat TN, Weissig H, Shindyalov IN, Bourne PE. The Protein Data Bank. *Nucleic Acids Res.* 2000; 28: 235-242.

[2] Molecular Operating Environment (MOE). 2015, Chemical Computing Group ULC: 1010 Sherbooke St. West, Suite #910, Montreal, QC, Canada.

[3] Jones G, Willett P, Glen RC, Leach AR, Taylor R. Development and validation of a genetic algorithm for flexible docking. *J. Mol. Biol.* 1997; 267: 727-748.

[4] Wolber G, Langer T. LigandScout: 3-D Pharmacophores derived from protein-bound ligands and their use as virtual screening filters. *J. Chem. Inf. Model.* 2005; 45: 160-169.

[5] Wolber G, Dornhofer AA, Langer T. Efficient overlay of small organic molecules using 3D pharmacophores. *J. Comput. Aided Mol. Des.* 2006; 20: 773-788.

[6] Balestri F, Cappiello M, Moschini R, Rotondo R, Buggiani I, Pelosi P, Mura U, Del Corso A. L-Idose: an attractive substrate alternative to D-glucose for measuring aldose reductase activity. *Biochem. Biophys. Res. Commun.* 2015; 456: 891-895.

[7] Balestri F, Cappiello M, Moschini R, Rotondo R, Abate A, Del Corso A, Mura U. Modulation of aldose reductase activity by aldose hemiacetals. *Biochim. Biophys. Acta* 2015; 1850: 2329-2339.

[8] Morrison JF. Kinetics of the reversible inhibition of enzyme-catalysed reactions by tight-binding inhibitors. *Biochim. Biophys. Acta* 1969; 185: 269-286.